Acta Oceanol. Sin., 2025, Vol. 44, No. 1, P. 50–58
https://doi.org/10.1007/s13131-024-0002-3

Empirical relationship between significant wave period and wave energy period in the coastal waters of China

Yuhuan Xue[1], Chuanjiang Huang[1, 2, 3*], Gang Wang[1, 2, 3], Dejun Dai[1, 2, 3], Fangli Qiao[1, 2, 3]

[1] First Institute of Oceanography, Ministry of Natural Resources, Qingdao 266061, China
[2] Laboratory for Regional Oceanography and Numerical Modeling, Qingdao Marine Science and Technology Center, Qingdao 266237, China
[3] Key Laboratory of Marine Science and Numerical Modeling, Ministry of Natural Resources, Qingdao 266061, China

Received 3 July 2024; accepted 30 November 2024

Abstract
Significant wave period is an important parameter in coastal and offshore engineering design. Traditional spectral wave models do not directly calculate this parameter, which means that it needs to be estimated from the spectral periods using empirical formulas. The wave energy period is one of the wave periods directly output by many wave models and is often used in studies of wave energy. This study investigated the relationship between significant wave period and wave energy period using wave data measured at three stations in the coastal waters of China. The observations recorded at these stations in the South China Sea, the East China Sea, and the Bohai Sea covered a wide range of surface wave conditions. Analysis indicated that the ratio of significant wave period to wave energy period is closely related to the Goda peakedness parameter of the wave spectra. Therefore, we proposed an empirical formula in which significant wave period is a function of wave energy period and the Goda peakedness parameter. Evaluation results showed that the performance of this formula is substantially better than that of fitting formulas that use constant coefficients.

Key words surface waves, significant wave period, wave energy period, wave spectral parameter, wave spectra

Citation Xue Yuhuan, Huang Chuanjiang, Wang Gang, Dai Dejun, Qiao Fangli. 2025. Empirical relationship between significant wave period and wave energy period in the coastal waters of China. Acta Oceanologica Sinica, 44(1): 50–58, doi: 10.1007/s13131-024-0002-3

1 Introduction

Surface waves have notable impact on coastal and offshore structures (Goda, 2010; Xu et al., 2022; Sun et al., 2023) and on processes at the air-sea interface (Drennan et al., 2003; Huang and Qiao, 2021). Due to the limitations of observation conditions and engineering costs, numerical wave models are often used to estimate wave parameters in ocean engineering design. Although wave models have made considerable progress in the past few decades (Cavaleri et al., 2007; Roland and Ardhuin, 2014), traditional wave models have been developed using energy balance analysis (Yuan and Huang, 2012). Consequently, such models simulate the spectral distribution of wave energy rather than the sea surface height, from which almost all wave parameters are then derived by the spectral analysis.

Significant wave period (T_s), defined as the mean period of one-third of the highest waves, is an important parameter used to characterize waves. However, because this parameter is obtained from the zero-crossing analysis of sea surface heights, it is not predicted by traditional spectral wave models (Chun and Suh, 2018). Therefore, it often needs to be estimated from the spectral periods using empirical formulas.

In order to describe different statistical and physical characteristics of waves, there are various commonly used spectral period parameters, including the peak period T_p, zero-crossing period T_{m02} ($=\sqrt{m_0/m_2}$), mean period T_{m01} ($=m_0/m_1$), and wave energy period $T_{m-1,0}$ ($=m_{-1}/m_0$), where $m_n=\int_0^\infty f^n S(f)\mathrm{d}f$ is the n-th moment of the wave power spectral density function $S(f)$, and f is the frequen-

Foundation item: The National Natural Science Foundation of China under contract No. 41821004; the Basic Scientific Fund for National Public Research Institutes of China under contract No. 2020Q08; the Fund of Laoshan Laboratory under contract No. LSKJ202201600.
*Corresponding author, E-mail: cjhuang@fio.org.cn

cy (Cuadra et al. 2016; ECMWF, 2021). Many studies have investigated the relationship between different wave periods, most of which were based on simple linear analysis (Holthuijsen, 2007; Li, 2007; Suh et al., 2010; Huang et al., 2016; Ahn, 2021; Kumar and Mandal, 2022), but there were also some studies suggesting that their relationship is related to the spectral characteristics of waves (Goda, 2010; Chun and Suh, 2018). Overall, there are significant differences in the relationship between different wave periods in these studies (Li, 2007; Goda, 2010; Huang et al., 2016), and then there is still much room for studies of wave periods.

On the basis of *in situ* observation data, laboratory data, and simulation data, Li (2007) argued that the relationship between T_s and the spectral periods calculated from the negative moment of the spectrum was more stable compared to other spectral periods. Using wave data from the Sea of Japan, Chun and Suh (2018) found that the formula using $T_{m-1,0}$ produced the best fitting result for T_s. The $T_{m-1,0}$, also known as the wave energy period (T_e), is one of the mean wave periods directly output by many wave models (WW3DG, 2019; ECMWF, 2021) and is often used in studies on wave energy (Bouferrouk et al., 2016; Cuadra et al., 2016). It is more stable than the peak period, especially for sea states where wind waves and swells coexist, and it is less sensitive than other commonly used wave periods (such as T_{m02} and T_{m01}) to the high-frequency cutoff of the spectrum (Jiang et al., 2022; Anju et al., 2023; Muraleedharan et al., 2023).

In this study, we examined the relationship between T_s and T_e using wave data measured at three stations in the coastal waters of China, and we proposed an empirical formula for calculating T_s using T_e. The remainder of the paper is structured as follows. The data and methods used in the study are described in Section 2. The derived empirical formula and the evaluation results are presented in Section 3. Finally, our conclusions are provided in Section 4.

2 Data and methods

2.1 *Wave data*

The observations were conducted in the South China Sea (SCS), East China Sea (ECS), and Bohai Sea (BS) (Fig. 1), where the surface waves were measured through acoustic surface tracking using acoustic Doppler current profilers (ADCPs) fixed to bottom-mounted frames. The observation station in the SCS is at 21.44°N, 111.39°E (Table 1). The location is approximately 6.5 km from the nearest shore, with a mean water depth of 16 m. The observational period extended from February 23, 2017, to August 1, 2017, during which a 1 000 kHz ADCP (Nortek Signature 1000) was deployed to measure surface waves. Its sampling time was set to 1 024 s per hour, and the output wave spectrum was in the range of 0.02–0.99 Hz with a resolution of 0.01 Hz.

The observation station in the ECS is at 27.68°N, 121.35°E. The location is approximately 25 km from the coast, with a mean water depth of 28 m. The observational period extended from June 4, 2017, to September 13, 2017. The observation station in the BS is at 38.31°N, 118.91°E. The location is approximately 19 km from the coast, with a mean water depth of 19 m. The observational period extended from December 19, 2022, to March 31, 2023. At the ECS and BS stations, 1 000 kHz ADCPs (Nortek AWAC) were used to measure surface waves. The sampling time was also set to 1 024 s per hour, but the wave spectral range was 0.02–1.99 Hz with a resolution of 0.01 Hz.

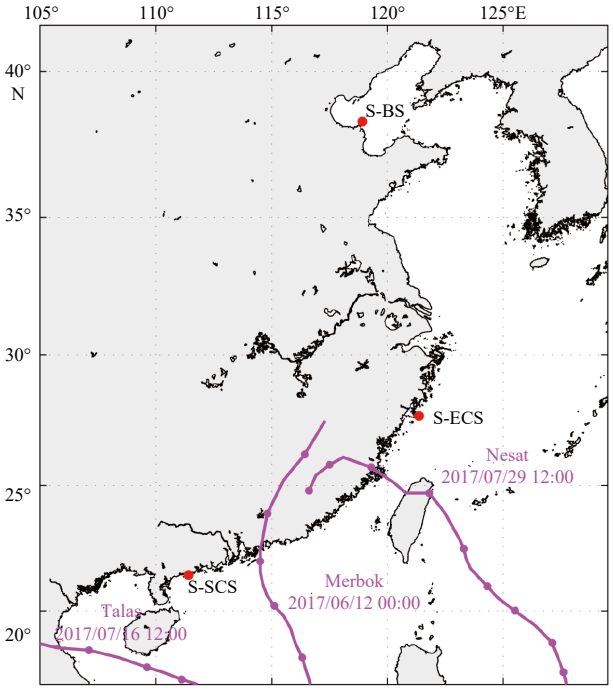

Fig. 1. Locations of three wave measurement stations (red dots) in the coastal waters of China. Pink curves are the tracks of Typhoons Merbok, Talas, and Nesat in 2017, respectively.

Table 1. Information on the three observation stations

Station	Location	Water depth/m	Distance to land/km	Data period (year/month/day)	Instrument	Spectral range/Hz
S-SCS	21.44°N, 111.39°E	16	6.5	2017/02/23–2017/08/01	Signature 1000	0.02–0.99
S-ECS	27.68°N, 121.35°E	28	25.0	2017/06/04–2017/09/13	AWAC	0.02–1.99
S-BS	38.31°N, 118.91°E	19	19.0	2022/12/19–2023/03/31	AWAC	0.02–1.99

Note: The sampling time for these observations was 1 024 s per hour, and the resolution of the wave spectra was 0.01 Hz.

2.2 *Evaluation method*

Following previous studies (Jiang et al., 2022; Bujak et al., 2023), the metrics of bias, root mean square error (RMSE), and correlation coefficient (COR) were used to evaluate the performance of the empirical formulas for the relationship between different wave periods. The formulas for calculation of these metrics can be expressed as follows:

$$\text{Bias} = \frac{1}{N}\sum_{i=1}^{N}(P_i - O_i), \tag{1}$$

$$\text{RMSE} = \sqrt{\frac{1}{N}\sum_{i=1}^{N}(P_i - O_i)^2}, \tag{2}$$

$$\text{COR} = \frac{\sum_{i=1}^{N}(P_i - \overline{P})(O_i - \overline{O})}{\left[\sqrt{\sum_{i=1}^{N}(P_i - \overline{P})^2}\right]\left[\sqrt{\sum_{i=1}^{N}(O_i - \overline{O})^2}\right]}, \tag{3}$$

where O represents the observed wave period, P represents the wave period modelled using empirical formulas, and N represents the number of available observation data points.

3 Empirical formulas and evaluation results

3.1 *Surface wave conditions*

China's coastal waters are affected by monsoons, cold fronts, typhoons, and other factors that create complex and variable surface wave conditions. The SCS is controlled by the Southeast Asian monsoon system. Our observations in this region, conducted in February–August, were affected first by the winter monsoon and then by the summer monsoon. Overall, the observed surface waves were dominated by swells, with significant wave heights in the range of 0.3–1.5 m and T_s in the range of 3–7 s. However, during the observational period, the passage of two severe tropical storm processes resulted in a long T_s of 8.9 s on June 12 and a large significant wave height of 2.4 m on July 16 (Figs 2a and b).

Our observations in the ECS were obtained in sum-

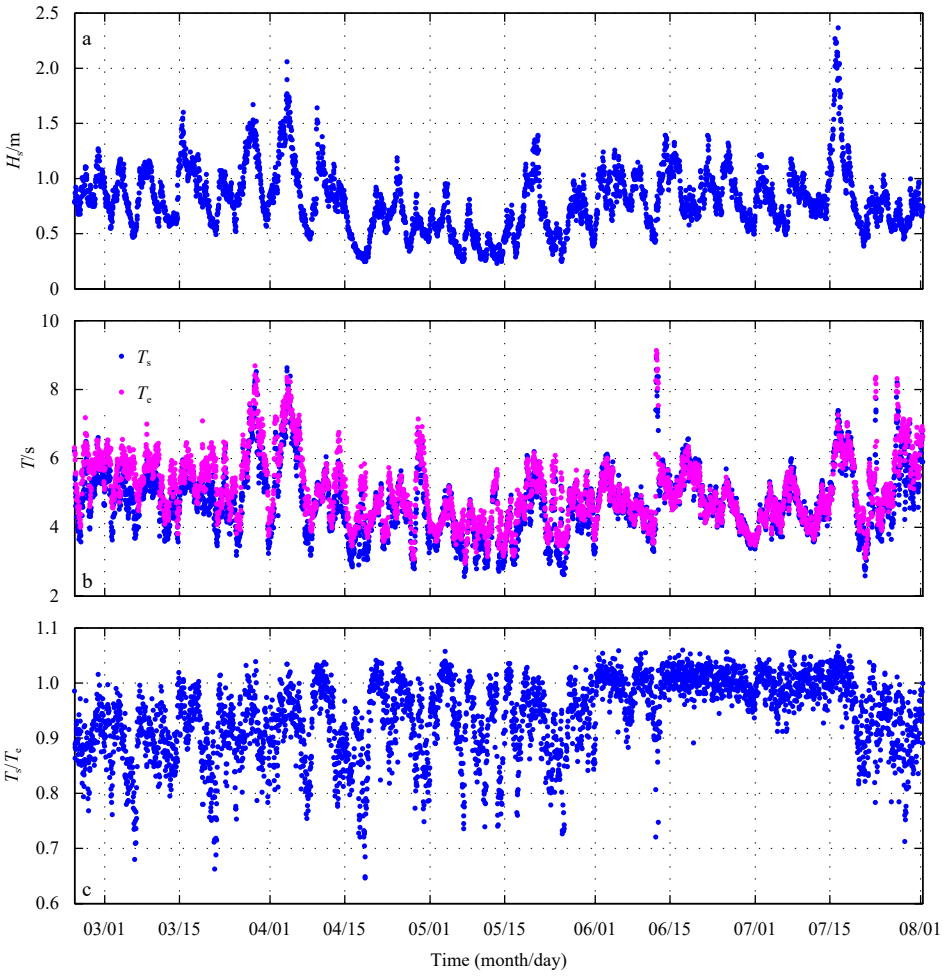

Fig. 2. Time series of significant wave height (a), period (b), and ratio of T_s to T_e (c) observed in the South China Sea during February–August 2017. In b, blue dots and pink dots represent significant wave period T_s and wave energy period T_e, respectively

mer, when the sea area is susceptible to the influence of typhoons. During our observation period, owing to the influence of Typhoon Nesat, the maximum significant wave height exceeded 5 m, and the maximum T_s exceeded 12 s (Figs 3a and b).

The BS is a shallow, semi-enclosed marginal sea where the surface waves are dominated by wind waves. During our observational period, approximately 81% of the valid data segments had a significant wave height of less than 1 m and T_s of less than 5 s. However, owing to the influence of winter cold fronts, there were also some observational segments with significant wave heights of larger than 3 m and T_s of larger than 7 s (Figs 4a and b).

Previous studies typically used linear fitting with constant coefficients to examine the relationship between different wave periods (Li, 2007; Huang et al., 2016; Ahn, 2021). Figure 5 shows scatter plots of T_s and T_e measured at the three stations, together with their linear fitting formulas in the form of $T_s = \alpha T_e$, where α is a constant. It is evident that the coefficient of the linear fitting of these two parameters is not the same at each of the three stations. In the SCS, dominated by swells, the value of coefficient α is 0.95, whereas it is 0.99 in the BS. This finding is similar to that of previous studies on fitting wave periods, where different fitting coefficients are usually obtained when using different observational datasets (Li, 2007; Ahn, 2021). It means that the constant coefficient fitting method has a certain dependence on local wave characteristics, which to some extent limits the applicability of this fitting method.

3.2 *Empirical formula derived from wave data in the SCS*

Although T_s compares well with T_e for each of the three observation datasets (Figs 2b, 3b, and 4b), the ratio of the two parameters (i.e., T_s/T_e) varies greatly, both spatially and temporally, in the range of 0.40–1.07 (Figs 2c, 3c, and 4c). This variation might be related to the wave spectral characteristics at the three stations. The Goda peakedness parameter (see ECMWF, 2021), which is an important parameter often used to represent wave spectral characteristics (Fairley et al., 2020; Le Merle et al., 2021), can be calculated directly using the wave spectrum as follows:

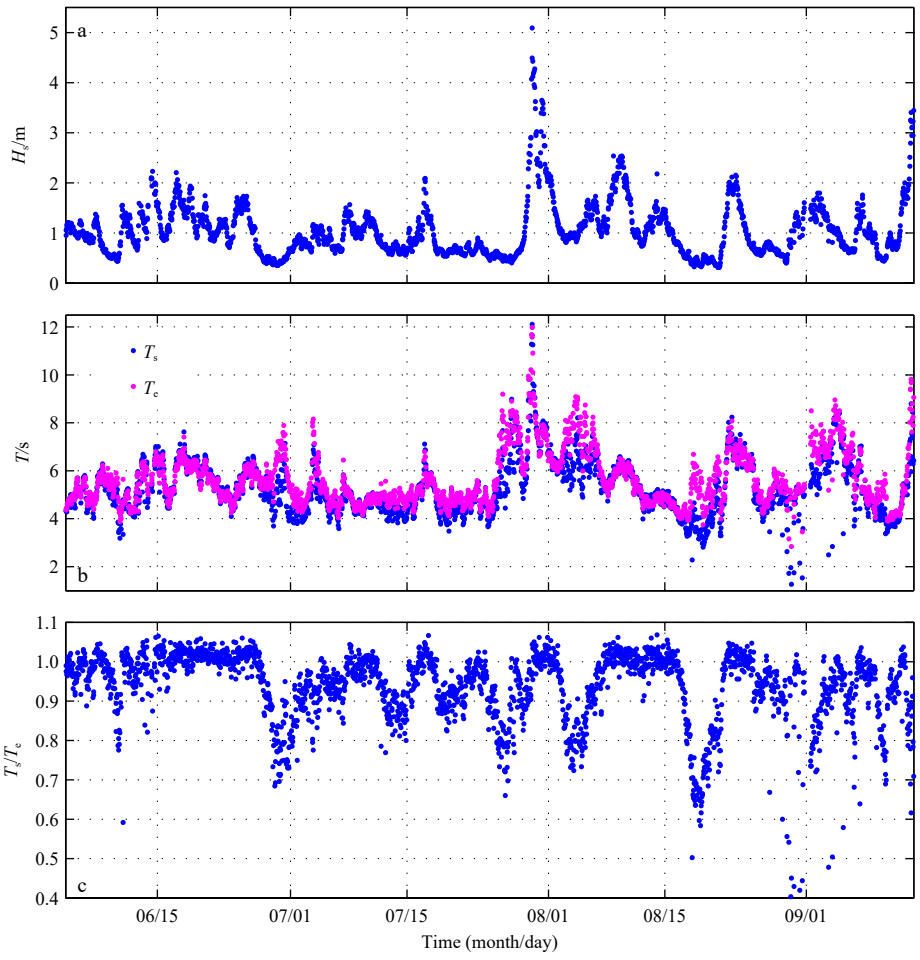

Fig. 3. Time series of significant wave height (a), period (b), and ratio of T_s to T_e (c) observed in the East China Sea during June–September 2017. In b, blue dots and pink dots represent significant wave period T_s and wave energy period T_e, respectively

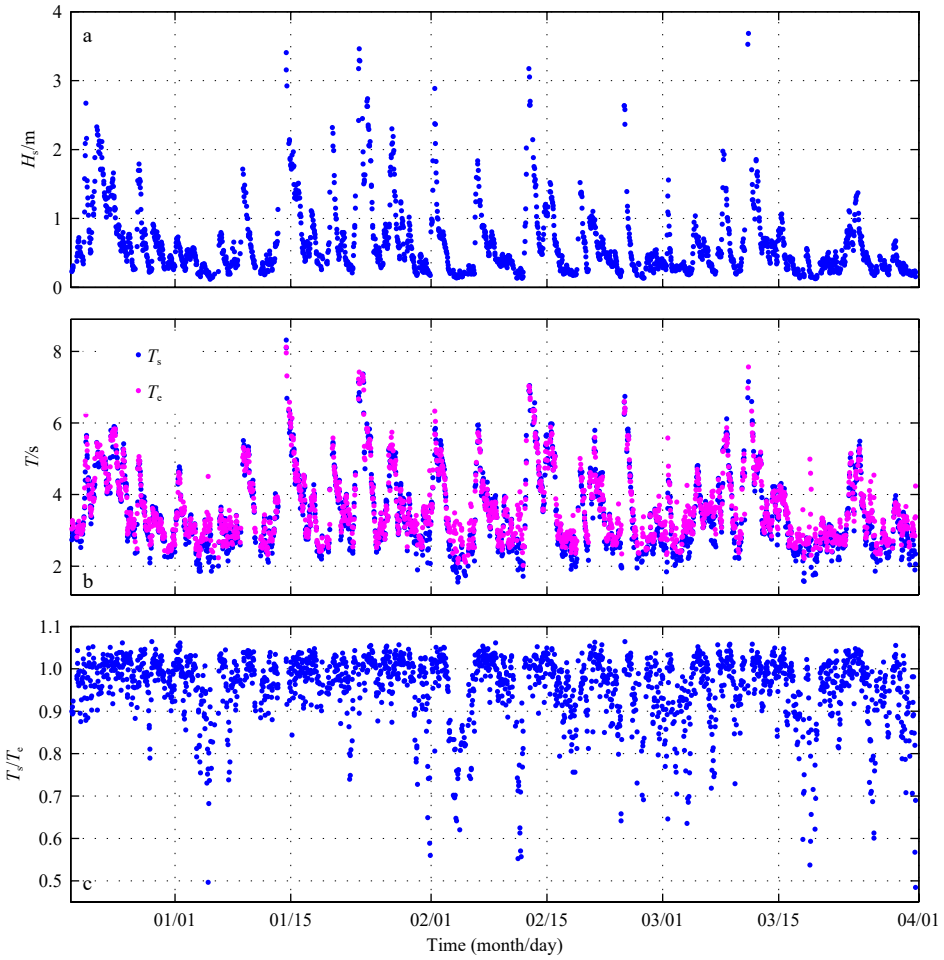

Fig. 4. Time series of significant wave height (a), period (b), and ratio of T_s to T_e (c) observed in the Bohai Sea during December 2022 to March 2023. In b, blue dots and pink dots represent significant wave period T_s and wave energy period T_e, respectively

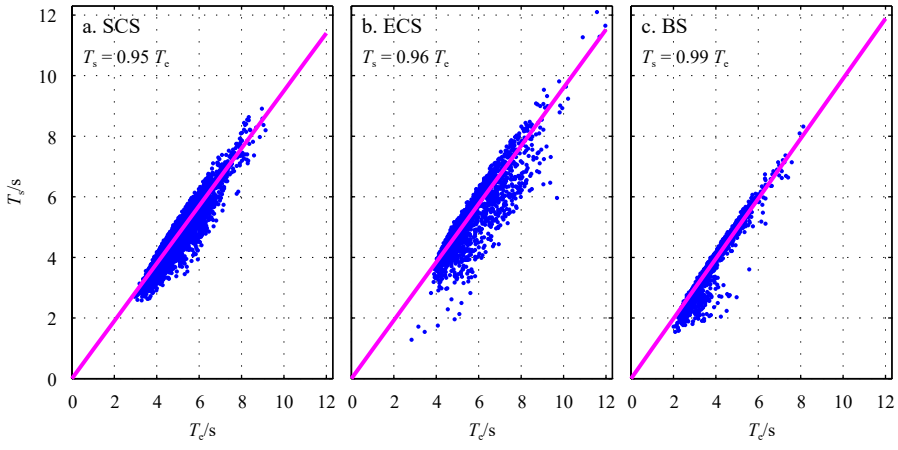

Fig. 5. Scatter plots of significant wave period T_s against wave energy period T_e measured in the South China Sea (SCS) (a), the East China Sea (ECS) (b), and the Bohai Sea (BS) (c). Pink lines represent the linear regressions of T_e on T_s in each panel.

$$Q_p = \frac{2}{m_0^2}\int_0^\infty fS^2(f)\,\mathrm{d}f. \tag{4}$$

This parameter is a measure of the sharpness of the wave spectrum, where larger Q_p usually correspond to narrower spectra (or more sharply peaked spectra), and vice versa. Compared to other commonly used wave bandwidth parameters, it is more reliable because of the stable quantities such as m_0 and $S(f)$ used in its calculation, and it is independent of the high-frequency cutoff

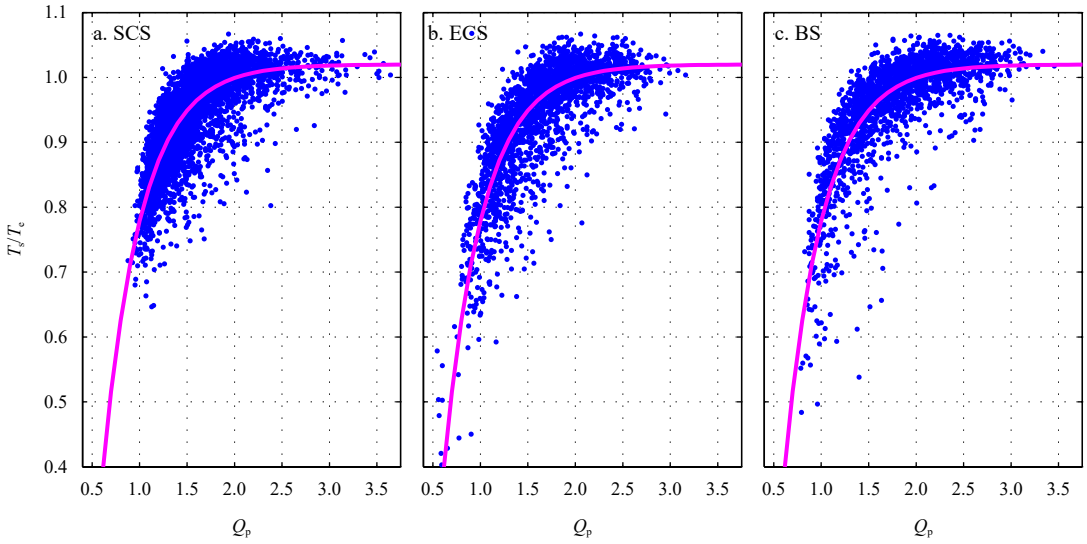

Fig. 6. Scatter plot of the ratio of significant wave period T_s and wave energy period T_e as a function of the Goda peakedness parameter Q_p for wave data in the South China Sea (SCS) (a), the East China Sea (ECS) (b), and the Bohai Sea (BS) (c). Pink curves are exponential fits using Eq. (5).

choice of the spectrum (Prasada Rao, 1988). It has been used to fit the relationship between T_s and the peak period by Chun and Suh (2018) and to predict wave runup on beaches by Bujak et al. (2023).

Figure 6a shows the relationship between the ratio of T_s to T_e and Q_p derived from the wave data obtained in the SCS. Overall, this ratio varies approximately exponentially with Q_p. It is slightly larger than 1 when Q_p is greater than 2 and decreases rapidly with Q_p when the latter is less than 2. Therefore, on the basis of the least squares method, we proposed the following empirical regression model:

$$T_s = \left[1.02 - 2.8\exp(-2.49Q_p)\right]T_e. \quad (5)$$

The performance of this formula and that of the constant coefficient linear fitting formula (see Fig. 5a) are respectively shown in Figs 7a and d. For wave data in the SCS, the bias, RMSE, and COR between the T_s modelled using the linear fitting formula and the observations are 0.052 s, 0.360 s, and 0.930, respectively (Table 2). However, when using Eq. (5), the bias and RMSE decreased to 0.010 s and 0.230 s, respectively, while the COR increased to 0.970, i.e., all markedly improved relative to the linear fitting results.

3.3 *Validation of the formula using wave data from the ECS and the BS*

The sea conditions in the ECS and BS are different to those in the SCS (Figs 2–4), but the relationship of the ratio of T_s to T_e with Q_p in the ECS and BS is fairly consistent with that in the SCS (Figs 6b and c). In the ECS, the bias, RMSE, and COR between the T_s modelled using the linear fitting formula (Fig. 5b) and the observed data are 0.136 s, 0.54 s, and 0.88, respectively (Fig. 7b). However, when using Eq. (5) including Q_p, the bias and RMSE between them decreased to 0.003 s and 0.29 s, respectively, and the COR increased to 0.97 (Fig. 7e). In the BS, the bias, RMSE, and COR between the T_s modelled using the linear fitting formula (Fig. 5c) and the observed data are 0.093 s, 0.29 s, and 0.96, respectively (Fig. 7c). However, when using Eq. (5), the bias and RMSE between them decreased to −0.004 s and 0.18 s, respectively, and the COR increased to 0.99 (Fig. 7f). These improvements demonstrate the applicability of our derived formula [i.e., Eq. (5)] to the coastal waters of China.

3.4 *Comparison with previous fitting formulas*

Using *in situ* observations from the BS, laboratory data, and simulation data, Li (2007) derived a linear empirical formula for fitting T_s using T_e, which can be expressed as follows:

$$T_s = 1.035T_e. \quad (6)$$

For our three sets of wave observations, the ratio of T_s to T_e is in the range 0.40–1.07. Therefore, although the fitting coefficient of Li (Li, 2007) is greater than ours (Fig. 5), it is still within the range of our observed ratios.

Using wave data from the Sea of Japan, Chun and Suh (2018) estimated T_s as follows:

$$T_s = 0.76T_e^{1.11}. \quad (7)$$

Figures 7g–l show scatter plot comparisons between the T_s modelled by the above two formulas and our measured T_s in the SCS, ECS, and BS. The results show that the performance of our derived formula [i.e., Eq. (5)] is substantially better than that of the other two formulas in relation to our wave data obtained in the coastal waters of

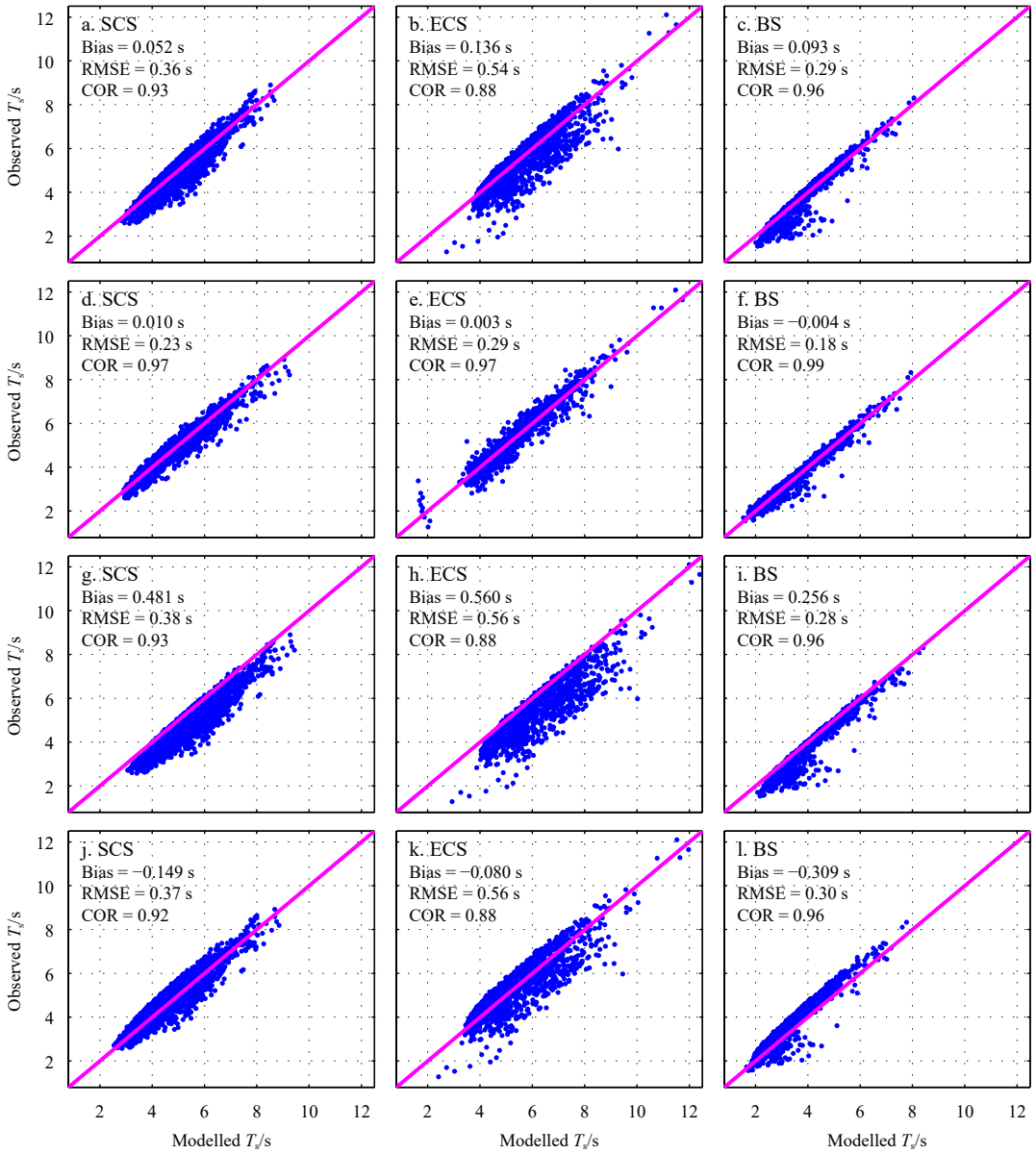

Fig. 7. Scatter plots comparing the observed significant wave period T_s and modelled T_s using different formulas for wave data from the South China Sea (SCS) (the left column), the East China Sea (ECS) (the middle column), and the Bohai Sea (BS) (the right column). The panels in the top, second, third, and bottom rows correspond to the comparison for linear fitting with constant coefficients in Fig. 5, Eq. (5), Eq. (6), and Eq. (7), respectively. Pink lines represent the 1:1 fittings.

Table 2. Statistical comparisons of the significant wave period modelled by different empirical formulas relative to the observations

Formulas		Linear fitting in Fig. 5	Eq. (5)	Eq. (6)	Eq. (7)
SCS	Bias/s	0.052	0.01	0.481	–0.149
	RMSE/s	0.36	0.23	0.38	0.37
	COR	0.93	0.97	0.93	0.92
ECS	Bias/s	0.136	0.003	0.56	–0.08
	RMSE/s	0.54	0.29	0.56	0.56
	COR	0.88	0.97	0.88	0.88
BS	Bias/s	0.093	–0.004	0.256	–0.309
	RMSE/s	0.29	0.18	0.28	0.30
	COR	0.96	0.99	0.96	0.96

China (Table 2).

4 Conclusions

The wave period, together with the wave height, is an important parameter in ocean engineering and physical oceanography. Compared to other wave spectral periods, the wave energy period is relatively stable and less sensitive to high-frequency cutoff of the spectrum, and it is also one of the wave periods directly output by many wave modes. In this study, we investigated the relationship between the significant wave period and wave energy period using wave data measured at three stations in the SCS, ECS, and BS.

In our observational data, although the two wave periods might appear similar, the ratio between them varies greatly. Therefore, traditional linear fitting using constant coefficients does not provide robust and universally applicable results. We found that this ratio is closely related to the Goda peakedness parameter of wave spectra. Therefore, we proposed an empirical formula for their relationship. Evaluation results showed that the performance of this proposed formula is notably better than that of both traditional linear fitting using constant coefficients and several empirical formulas presented in previous studies.

In addition to the wave energy period, other spectral periods are commonly used in wave studies (Cuadra et al., 2016). Although their performance is not as robust as that of the wave energy period, they do represent the spectral characteristics of waves from different aspects. In future studies, we will examine the relationship between significant wave period and these other spectral periods.

References

Ahn S. 2021. Modeling mean relation between peak period and energy period of ocean surface wave systems. Ocean Engineering, 228: 108937, doi: 10.1016/j.oceaneng.2021.108937

Anju T M, Kumar V S, Singh J, et al. 2023. Period and length of high surface gravity waves measured in the coastal waters of eastern Arabian Sea and its variations in 10 years. Regional Studies in Marine Science, 67: 103224, doi: 10.1016/j.rsma.2023.103224

Bouferrouk A, Saulnier J B, Smith G H, et al. 2016. Field measurements of surface waves using a 5-beam ADCP. Ocean Engineering, 112: 173–184, doi: 10.1016/j.oceaneng.2015.12.025

Bujak D, Ilic S, Miličević H, et al. 2023. Wave runup prediction and alongshore variability on a pocket gravel beach under fetch-limited wave conditions. Journal of Marine Science and Engineering, 11(3): 614, doi: 10.3390/jmse11030614

Cavaleri L, Alves J H G M, Ardhuin F, et al. 2007. Wave modelling: The state of the art. Progress in Oceanography, 75(4): 603–674, doi: 10.1016/j.pocean.2007.05.005

Chun H, Suh K D. 2018. Estimation of significant wave period from wave spectrum. Ocean Engineering, 163: 609–616, doi: 10.1016/j.oceaneng.2018.06.043

Cuadra L, Salcedo-Sanz S, Nieto-Borge J C, et al. 2016. Computational intelligence in wave energy: Comprehensive review and case study. Renewable and Sustainable Energy Reviews, 58: 1223–1246, doi: 10.1016/j.rser.2015.12.253

Drennan W M, Graber H C, Hauser D, et al. 2003. On the wave age dependence of wind stress over pure wind seas. Journal of Geophysical Research: Oceans, 108(C3): 8062, doi: 10.1029/2000JC000715

ECMWF. 2021. IFS documentation Cy47r3. Part Ⅶ: ECMWF wave model. Reading, UK: ECMWF, https://www.ecmwf.int/node/20201 [2021-10-12/2024-5-18]

Fairley I, Lewis M, Robertson B, et al. 2020. A classification system for global wave energy resources based on multivariate clustering. Applied Energy, 262: 114515, doi: 10.1016/j.apenergy.2020.114515

Goda Y. 2010. Random Seas and Design of Maritime Structures. 3rd ed. Singapore: World Scientific Publishing, 17–188

Holthuijsen L H. 2007. Waves in Oceanic and Coastal Waters. Cambridge: Cambridge University Press, 60–75

Huang Bigui, Shi Xingang, Xie Botao, et al. 2016. Study on the relationships of ocean wave periods in the South China Sea based on the observed data. Journal of Marine Sciences (in Chinese), 34(3): 6–10, doi: 10.3969/j.issn.1001-909X.2016.03.002

Huang Chuanjiang, Qiao Fangli. 2021. Simultaneous observations of turbulent Reynolds stress in the ocean surface boundary layer and wind stress over the sea surface. Journal of Geophysical Research: Oceans, 126(2): e2020JC016839, doi: 10.1029/2020JC016839

Jiang Haoyu, Song Yuhao, Mironov A, et al. 2022. Accurate mean wave period from SWIM instrument on-board CFOSAT. Remote Sensing of Environment, 280: 113149, doi: 10.1016/j.rse.2022.113149

Kumar V S, Mandal S. 2022. Characteristics of individual surface waves measured by moored buoys in the coastal waters of the eastern Arabian Sea. Ocean Engineering, 248: 110861, doi: 10.1016/j.oceaneng.2022.110861

Le Merle E, Hauser D, Peureux C, et al. 2021. Directional and frequency spread of surface ocean waves from SWIM measurements. Journal of Geophysical Research: Oceans, 126(7): e2021JC017220, doi: 10.1029/2021JC017220

Li Ruili. 2007. On the relationships of various wind wave periods. Transactions of Oceanology and Limnology (in Chinese), (2): 13–18, doi: 10.3969/j.issn.1003-6482.2007.02.003

Muraleedharan G, Lucas C, Soares C G. 2023. Spectral wave energy period and peak period statistics concomitant with maximum significant wave heights. Coastal Engineering, 183: 104260, doi: 10.1016/j.coastaleng.2022.104260

Prasada Rao C V K. 1988. Spectral width parameter for wind-generated ocean waves. Proceedings of the Indian Academy of Sciences–Earth and Planetary Sciences, 97(2):

173–181, doi: 10.1007/BF02861852

Roland A, Ardhuin F. 2014. On the developments of spectral wave models: numerics and parameterizations for the coastal ocean. Ocean Dynamics, 64(6): 833–846, doi: 10.1007/s10236-014-0711-z

Suh K D, Kwon H D, Lee D Y. 2010. Some statistical characteristics of large deep water waves around the Korean Peninsula. Coastal Engineering, 57(4): 375–384, doi: 10.1016/j.coastaleng.2009.10.016

Sun Qi, Chen Diyu, Luo Zhao. 2023. Dynamic response studies and mooring system optimization of a piling ship under long and medium period waves in deep waters. China Harbour Engineering (in Chinese), 43(5): 25–29,56, doi: 10.7640/zggwjs202305005

WW3DG. 2019. User manual and system documentation of WAVEWATCH III® version 6.07. College Park: NOAA/NWS/NCEP/MMAB, https://www.weather.gov/sti/coastalact_ww3[2019-3-21/2024-5-20]

Xu Yaoyao, Qu Ke, Huang Jingxuan, et al. 2022. Numerical simulation of wave dissipation characteristics of permeable submerged breakwater under focused wave. Haiyang Xuebao (in Chinese), 44(11): 121–132, doi: 10.12284/hyxb2022127

Yuan Yeli, Huang N E. 2012. A reappraisal of ocean wave studies. Journal of Geophysical Research: 117(C11): C00J27, doi: 10.1029/2011JC007768